Diagnostic performance of myocardial perfusion imaging with conventional and CZT single-photon emission computed tomography in detecting coronary artery disease: A meta-analysis

Valeria Cantoni, PhD,[a] Roberta Green, PhD,[a] Wanda Acampa, MD, PhD,[a,b] Emilia Zampella, MD, PhD,[a] Roberta Assante, MD, PhD,[a] Carmela Nappi, MD, PhD,[a] Valeria Gaudieri, MD, PhD,[a] Teresa Mannarino, MD,[a] Renato Cuocolo, MD,[a] Eugenio Di Vaia, MD,[a] Mario Petretta, MD, FAHA,[c] and Alberto Cuocolo, MD[a]

[a] Department of Advanced Biomedical Sciences, University Federico II, Naples, Italy
[b] Institute of Biostructure and Bioimaging, National Council of Research, Naples, Italy
[c] Department of Translational Medical Sciences, University Federico II, Naples, Italy

Received Mar 5, 2019; accepted Apr 23, 2019
doi:10.1007/s12350-019-01747-3

Background. **We performed a meta-analysis to compare the diagnostic performance of conventional SPECT (C-SPECT) and cadmium-zinc-telluride (CZT)-SPECT systems in detecting angiographically proven coronary artery disease (CAD).**

Methods. **Studies published between January 2000 and February 2018 were identified by database search. We included studies assessing C-SPECT or CZT-SPECT as a diagnostic test to evaluate patients for the presence of CAD, defined as at least 50% diameter stenosis on invasive coronary angiography. A study was eligible regardless of whether patients were referred for suspected or known CAD.**

Results. **We identified 40 eligible articles (25 C-SPECT and 15 CZT-SPECT studies) including 7334 patients (4997 in C-SPECT and 2337 in CZT-SPECT studies). The pooled sensitivity and specificity were 85% and 66% for C-SPECT and 89% and 69% for CZT-SPECT imaging studies. The area under the curve was slightly higher for CZT-SPECT (0.89) compared to C-SPECT (0.83); accordingly, the summary diagnostic OR was 17 for CZT-SPECT and 11 for C-SPECT. The accuracy of the two tests slightly differs between C-SPECT and CZT-SPECT (chi-square 11.28, $P < .05$). At meta-regression analysis, no significant association between both sensitivity and specificity and demographical and clinical variables considered was found for C-SPECT and CZT-SPECT studies.**

Conclusions. **C-SPECT and CZT-SPECT have good diagnostic performance in detecting angiographic proven CAD, with a slightly higher accuracy for CZT-SPECT. This result supports**

Electronic supplementary material The online version of this article (https://doi.org/10.1007/s12350-019-01747-3) contains supplementary material, which is available to authorized users.

The authors of this article have provided a PowerPoint file, available for download at SpringerLink, which summarises the contents of the paper and is free for re-use at meetings and presentations. Search for the article DOI on SpringerLink.com.

All editorial decisions for this article, including selection of reviewers and the final decision, were made by guest editor Saurabh Malhotra, MD, MPH.

Valeria Cantoni and Roberta Green are the first two authors shared first co-authorship.

Reprint requests: Alberto Cuocolo, MD, PhD, Department of Advanced Biomedical Sciences, University Federico II, Via Pansini 5, 80131, Naples, Italy; *cuocolo@unina.it*

1071-3581/$34.00

the use of the novel gamma cameras in clinical routine practices also considering the improvements in acquisition time and radiation exposure reduction. (J Nucl Cardiol 2021;28:698–715.)

Key Words: CAD • SPECT • MPI • diagnostic application • meta-analysis

Abbreviations	
CAD	Coronary artery disease
MPI	Myocardial perfusion imaging
SPECT	Single-photon emission computed tomography
C	Conventional
CZT	Cadmium-zinc-telluride
OR	Odds ratio
CI	Confidence interval
ROC	Receiver operator characteristic

See related editorial, pp. 716–717

INTRODUCTION

Coronary artery disease (CAD) is still the leading cause of death in industrialized countries, and the prevalence is expected to increase worldwide.[1,2] In patients with known or suspected CAD, stress myocardial perfusion imaging (MPI) with single-photon emission computed tomography (SPECT) accounts for the vast majority of tests currently performed for ischemia detection. The diagnostic and prognostic role of this imaging modality is well established, and a negative stress MPI is able to identify subjects at low risk of future cardiovascular events.[3,4] However, conventional (C) SPECT (C-SPECT) systems utilize large sodium iodide crystals, photomultiplier tubes, and parallel-hole collimation and are therefore inherently insensitive, necessitating prolonged imaging times, and relatively large radioisotope doses. Recent innovations in camera technology, fast electronics, and reconstruction algorithms have addressed these issues.[5] The novel gamma cameras with semiconductor cadmium-zinc-telluride (CZT) detectors directly convert radiation into electric signals, allowing an improvement in terms of image accuracy and acquisition time.[6-8] Specifically, new multi-pinhole SPECT cameras with CZT solid-state detectors (CZT-SPECT) technology provide for faster image acquisition and lower radiation doses in comparison with traditional sodium-iodine Anger cameras. This allows for MPI protocols preserving diagnostic image quality and diagnostic accuracy.[9,10] At the best of our knowledge, the diagnostic performance of C-SPECT and CZT-SPECT have not been compared. Therefore, the aim of this meta-analysis was to compare the diagnostic performance of C-SPECT and CZT-SPECT systems in detecting CAD as defined by invasive coronary angiography.

MATERIALS AND METHODS

This meta-analysis followed the Preferred Reporting Items for Systematic Reviews and Meta-Analyses (PRISMA) statement (see the supplementary material for PRISMA checklist).[11]

Data Sources and Study Selection

We searched the PubMed and Web of Science databases for English literature from January 2000 to February 2018 on the diagnostic accuracy of MPI for the detection of CAD. Studies search was restricted to data obtained in humans and adults and was conducted using the following key words: myocardial perfusion imaging (OR MPI), single-photon emission tomography (OR SPECT), cadmium-zinc-telluride (OR CZT) SPECT, Anger camera and diagnostic performance in combination with coronary artery disease (OR CAD). The full search strategy for PubMed and Web of Science is shown in the supplementary material.

The bibliographies of selected articles and relevant reviews were screened for potentially suitable references. Two reviewers (V.C. and R.G.) screened for appropriateness title and abstract of potentially relevant studies and disagreement was resolved by consensus. The full-published reports of the abstracts selected by the reviewers were retrieved, and the same reviewers independently performed a second-step selection based on the inclusion criteria; disagreements were resolved by consensus. We included a study if: (1) it assessed C-SPECT or CZT-SPECT as a diagnostic test to evaluate patients for the presence of CAD; (2) CAD was defined as at least 50% diameter stenosis on invasive coronary angiography; and (3) it reported cases in absolute numbers of true positive, false positive, true negative, and false negative results, or if these data were derivable from the presented results. A study was eligible regardless of whether patients were referred for suspected or known CAD. Studies were excluded if they were conducted with: (1) phantom-only models and (2) study population without coronary angiographic correlation. In case of multiple studies reported from the same research group, potential cohort duplication was avoided by including the largest study only.

Data Extraction

Each study was initially identified considering author, journal and year of publication. Population data were collected on age, prevalence of female sex, traditional cardiovascular risk factors (diabetes, dyslipidemia, smoking, hypertension, family history of CAD), angina-like symptoms, and history of CAD (including previous myocardial infarction and coronary revascularization). Further extracted variables consisted of patient characteristics, technical information and absolute numbers of true negative, true positive, false negative, and

false positive test results. To improve the comparability of study results in the analysis of overall diagnostic performance, we selected a cut-off value of $\geq$ 50% whenever possible. However, if data were not reported for a cut-off value of $\geq$ 50%, we selected the cut-off value that was available (e.g. $\geq$ 70%). For C-SPECT, a cut-off of $\geq$ 50%% was used in 21 studies and a cut-off of $\geq$ 70% in 4 studies. For CZT-SPECT, a cut-off of $\geq$ 50%% was used in 10 studies and a cut-off of $\geq$ 70% in 5 studies.

Quality Assessment

The methodological assessments of the quality of eligible studies were graded by two reviewers independently, according to the Quality Assessment of Diagnostic Accuracy Studies 2 (QUADAS-2) tool (Agency for Healthcare Research and Quality, Cochrane Collaboration and the U.K. National Institute for Health and Care Excellence),[12] which is recommended for use in systematic reviews of diagnostic accuracy based on sources of bias and variation. The following four aspects are required to use the QUADAS-2 tool: (1) summarize the evaluation question; (2) develop the tool and produce evaluation with guidance; (3) construct a flow diagram for the original study; and (4) judge bias and applicability. The QUADAS-2 tool can provide obvious grades of bias and applicability of primary diagnostic accuracy studies. It comprises four significant domains including: (1) patient selection; (2) index test; (3) reference standard; and (4) the flow and timing. Each domain contains several signal questions used to help judge the risk of bias (low, high, or unclear).[12] The two reviewers completed the screening process independently. Disagreement in the process of answering questions was discussed until consensus was reached. A final decision of ''yes (favorable scenario, ''+'')'', ''no (unfavorable scenario, ''−'')'' or ''unclear (mixed scenario, ''+/−'')'' was made by the reviewers after systematic discussion. If the answers to all the signal problems were ''yes'', a low risk of bias was attributed to the study; if the answers to all the signal problems had one or more ''no'' or ''unclear'' values, an unclear risk of bias was used; if the answers to all the signal problems contained at least one ''no'' but no ''yes'' answers, a high risk of bias was attributed.

Statistical Analysis

For each eligible study, data were extracted to estimate sensitivity, specificity, and diagnostic odds ratio (OR) with 95% confidence interval (CI). The bivariate random-effects model was used to calculate the pooled summary estimates for sensitivities and specificities and to construct their forest plots for C-SPECT and CZT-SPECT.[13] The bivariate model estimates pairs of logit-transformed sensitivity and specificity from studies, incorporating the correlation that might exist between sensitivity and specificity. To measure the pooled accuracy, the parameters estimated by the bivariate model were used to construct a smooth summary receiver operator characteristic (ROC) curve, with the area under the curve and the summary operating point with the 95% confidence region calculated[13]; also, a prediction region that has a 95% probability of including true sensitivity and specificity of a future study was generated. The areas under the two summary ROC curves were compared using a formula provided by Hanley and McNeil.[14,15] Multilevel mixed-effects logistic regression was used to compare the summary paired sensitivity/specificity data, adding test type (C-SPECT or CZT-SPECT) as covariate. Likelihood ratio tests were used to obtain the statistical differences between the sensitivities and specificities of the two tests type by fitting alternative models, adding or removing the covariate term from the model.[16] Briefly, we compared the model without covariate with the including test-type as covariate allowing separate variances for each test. If a significant likelihood ratio test was found, to investigate if the difference in accuracy was due to sensitivity or specificity further analyses were done assuming the same sensitivity or specificity for the two test and dropping the relevant covariate terms from the model.[17] Between-study heterogeneity was evaluated with Cochran's Q and I^2 statistics. When statistical heterogeneity was substantial, meta-regression analysis was performed to identify potential confounders.[18] To evaluate the presence of diagnostic threshold effect, the correlation between sensitivity and specificity was examined by the Spearman rank correlation test. Publication bias was examined using the effective sample size funnel plot and associated regression test of asymmetry described by Deeks et al.[19] All analyses were performed using Stata, version 15.1 (StataCorp, College Station, TX). Two-sided P values $\leq$ .05 were considered statistically significant.

RESULTS

Search Results

The complete literature search is presented in Figure 1. The initial search identified 2973 potentially eligible citations. After removing 883 duplicate records, 2090 records were screened by the reviewers. After the titles and abstracts evaluation, 1877 citations were discharged because they were judged to be non-relevant or non-pertinent. Thus, 213 full-text articles were blinded assessed by each investigator for eligibility. After revision, 173 articles were excluded leaving 40 articles (25 C-SPECT and 15 CZT-SPECT studies) including 7334 patients (4997 in C-SPECT and 2337 in CZT-SPECT studies).

Characteristics of C-SPECT Studies

The characteristics of C-SPECT studies as well as demographic and clinical patient data are detailed in Table 1.[20-43] Data were obtained using exercise stress test in only one study,[23] exercise or pharmacologic stress test in 10 studies[22,24,26,28,32,35,36,41,42] and pharmacologic stress test in 14 studies.[20,21,25,27,28,30-32,34,37,38,40,43] The imaging tracers were Tc-99m labeled agents in 16

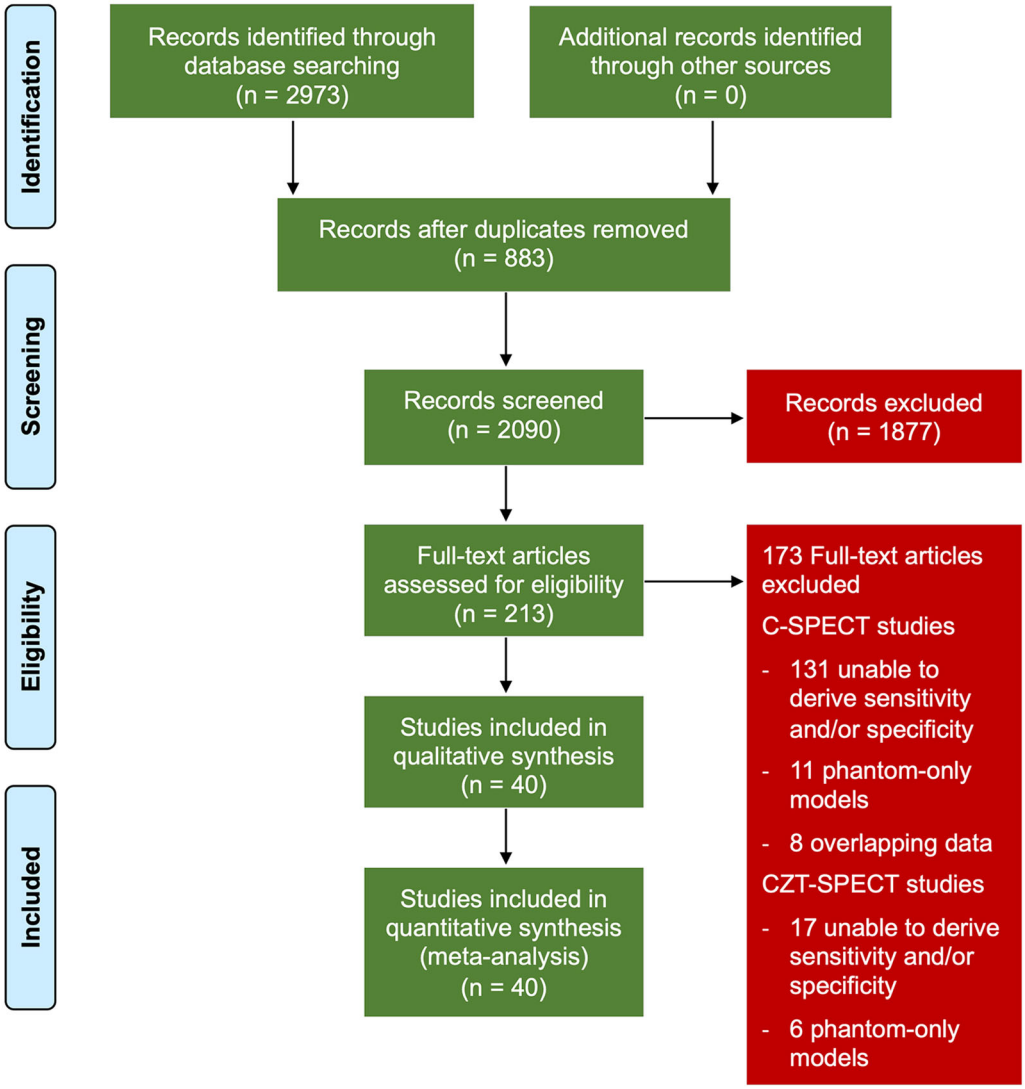

Figure 1. Literature search and selection process of studies included in analysis.

studies,[20-22,24,25,27,28,30,32-35,38,40,42,43] thallium-201 in 3 studies,[23,29,37] dual isotope thallium-201/Tc-99m sestamibi in 3 studies[26,31,41] and Tc-99m labeled agents or thallium-201 in 3 studies.[21,36,39] One study considered as cut-off of abnormality a summed stress score > 3,[42] 2 studies a summed stress score ≥ 4,[32,36] one study a summed stress score > 4.[41] One study considered as cut-off of myocardial ischemia summed difference score ≥ 2[35] while one study considered as cut-off of myocardial ischemia transient ischemic dilation ≥ 1.18.[43] In 7 studies, myocardial perfusion was defined normal when a perfusion defect involved < 3 myocardial segments.[20,21,23,24,26,33,39] In 2 studies, a normal response was defined as a normal uptake ($> 70\%$) at rest and after stressor injection.[27,31] Finally, in 10 studies the cut-off of abnormality was defined on visual analysis based on several different parameters.[22,25,28,30,34,37,38,40] Study sample size ranged from 31 to 1853 subjects. The mean age ranged from 56 to 72 years and the proportion of women from 8% to 100%. The diagnostic performance in detecting CAD for each study is shown in Table 2.

Characteristics of CZT-SPECT Studies

The characteristics of CZT-SPECT studies as well as demographic and clinical patient data are detailed in Table 3.[44–58] Data were obtained using exercise or pharmacologic stress test in 7 studies[45,46,48,50–52,57] and

Table 1. Demographic data and clinical characteristics of patients studied with C-SPECT camera

	Patients (*n*)	Age (years)	Women (%)	Diabetes (%)	Dyslipidemia (%)	Smoking (%)	Hyper-tension (%)	Angina (%)	Family history of CAD (%)	Prior MI (%)	Prior REV (%)
Elhendy[20]	124	57 ± 12	29	-	-	-	-	98	-	-	-
Smart[21]	183	60 ± 11	27	-	-	-	0	80	-	-	-
Kapur[22]	137	62 ± 12	-	-	-	-	-	-	-	-	-
Miller[22]	1853	63 ± 11	26	22	48	16	53	65	-	-	-
Tsai[23]	86	59 ± 9	17	19	-	59	49	-	93	36	-
Banzo[24]	99	59	28	-	-	-	-	-	-	-	
Doyle[25]	184	59 ± 11	100	-	-	-	-	-	-	-	-
Groutars[26]	123	61 ± 10	28	-	-	-	-	-	-	-	-
Peltier[27]	35	62 ± 10	28	17	45	34	66	77	-	-	20
Senior[28]	55	61	18	9	35	25	40	80	-	-	-
Sakuma[29]	40	65 ± 9	30	-	-	-	-	-	-	-	-
Squires[30]	50	60	53	-	-	-	-	-	-	-	-
Lin[31]	40	56	-	-	-	-	-	-	-	-	-
Berman[32]	785	67 ± 12	34	23	50	-	63	69	-	-	-
Jeetley[33]	123	62 ± 12	29	27	67	53	59	-	-	33	14
Korosoglou[34]	89	64 ± 9	49	-	-	-	-	-	-	-	-
Matsumoto[35]	56	62 ± 11	8	-	-	-	-	-	-	-	-
Weinsaft[36]	131	-	50	27	44	5	-	-	9	-	-
Yeih[37]	51	63 ± 9	100	-	-	-	-	-	-	-	
Lipiec[38]	103	58 ± 9	37	-	-	-	-	32	-	-	37
Tadehara[39]	101	72 ± 9	48	-	-	-	-	-	-	-	-
Wu[40]	218	64 ± 11	38	40	-	-	70	-	-	-	-
Shin[41]	246	61 ± 11	44	28	51	45	67	-	-	-	-
Patil[42]	54	66 ± 10	26	39	83	22	77	-	33	-	37
Ueki[43]	31	71 ± 8	16	29	55	52	77	-	13	10	26

CAD, coronary artery disease; *MI*, myocardial infarction; *Reva*, revascularization procedures

Table 2. Diagnostic performance in detecting coronary artery disease with C-SPECT camera

	True positive	False positive	True negative	False negative	Sensitivity (%)	Specificity (%)	Diagnostic odds ratio
Elhendy[20]	70	10	26	18	79.5	72.2	10.11
Smart[21]	95	17	47	24	79.8	73.4	10.94
Kapur[22]	86	10	33	8	91.4	76.7	35.47
Miller[22]	1307	449	65	32	97.6	12.6	5.91
Tsai[23]	60	11	12	3	95.2	52.2	21.82
Banzo[24]	47	26	22	4	92.2	45.8	9.94
Doyle[25]	16	28	130	10	61.5	82.3	7.43
Groutars[26]	101	6	9	7	93.5	60	21.64
Peltier[27]	18	2	11	4	81.8	84.6	24.75
Senior[28]	21	1	11	22	48.8	91.7	10.5
Sakuma[29]	17	7	12	4	81	63.2	7.29
Squires[30]	25	14	5	6	80.6	26.3	1.49
Lin[31]	19	3	12	6	76	80	12.67
Berman[32]	526	93	84	82	86.5	47.5	5.79
Jeetley[33]	79	13	14	17	82	52	5.00
Korosoglou[34]	48	13	14	14	77.4	51.9	3.69
Matsumoto[35]	22	1	29	4	84.6	96.6	159.5
Weinsaft[36]	49	34	35	13	79	50.7	3.88
Yeih[37]	20	3	20	8	71.4	87	16.67
Lipiec[38]	79	5	9	10	88.8	64.3	14.22
Tadehara[39]	50	14	33	4	92.6	70.2	29.46
Wu[40]	123	33	55	7	94.6	62.5	29.29
Shin[41]	140	34	53	19	88	61	11.49
Patil[42]	34	4	12	4	89	75	25.50
Ueki[43]	5	3	9	14	26	75	1.07

pharmacologic stress test in 8 studies.[44,47,49,53–56,58] The imaging tracer was a Tc-99m labeled agent in 10 studies,[44,46,49,51–53,55,56] thallium-201 in 2 studies,[57,58] dual isotope thallium-201/Tc-99m sestamibi in 2 studies[50,54] and Tc-99m sestamibi or thallium-201 in one study.[45] Two studies considered as cut-off of abnormality a summed stress score > 3,[53,57] 2 studies a summed stress score ≥ 4,[47,49] 2 studies considered as cut-off of myocardial ischemia summed difference score ≥ 2.[50,54] In 2 studies, myocardial perfusion was defined normal when a perfusion defect involved < 3 myocardial segments.[44,56] In 7 studies, the cut-off of abnormality was defined on 17-segment visual interpretation using a 5-point score.[45,46,48,50,52,55,58] Study sample size ranged from 44 to 695 subjects. The mean age ranged from 59 to 71 years and the proportion of women from 18% to 57%. The diagnostic performance in detecting CAD for each study is shown in Table 4.

Quality Assessment

The methodological quality assessment of risk of bias within eligible studies for C-SPECT is shown in Figure 2, according to the QUADAS-2 tool. Overall, the number of high, unclear, and low risk of bias was 1, 23, and 1, respectively, for the four domains (patient selection, index test, reference standard, and flow and timing). The number of unclear and low concerns regarding applicability was 22 and 3, respectively, for the three domains (patient selection, index test, and reference standard). The methodological quality assessment of risk of bias within eligible studies for CZT-SPECT is shown in Figure 3 according to the QUADAS-2 tool. Overall, the number of unclear and high risk of bias was 13 and 2, respectively, for the four domains (patient selection, index test, reference standard, and flow and timing). The number of unclear concerns regarding applicability was 15 for the three

Table 3. Demographic data and clinical characteristics of patients studied with CZT-SPECT camera

	Patients (*n*)	Age (years)	Women (%)	Diabetes (%)	Dyslipidemia (%)	Smoking (%)	Hyper-tension (%)	Angina (%)	Family history of CAD (%)	Prior MI (%)	Prior REV (%)
Fiechter[44]	66	63 ± 11	21	36	83	21	83	50	26	27	38
Duvall[45]	230	63 ± 12	31	40	81	53	80	74	19	-	49
Duvall[46]	71	64 ± 11	55	23	58	51	70	80	16	-	-
Chowdhury[47]	165	63 ± 9	-	-	-	-	-	-	-	-	-
Perrin[48]	149	64 ± 12	20	31	58	-	63	40	-	42	53
Nishiyama[49]	76	70 ± 10	39	33	47	47	67	28	22	12	36
Barone-Rochette[50]	104	65 ± 12	30	38	56	41	57	78	20	23	39
Mouden[51]	100	66 ± 10	36	31	65	-	67	-	-	-	-
Gimelli[52]	695	71 ± 11	23	33	43	11	60	77	28	20	12
Sharir[53]	208	61 ± 11	-	-	-	-	-	-	-	-	-
Caobelli[54]	44	65 ± 11	29	36	73	18	56	-	56	45	55
Liu[55]	211	59 ± 10	-	29	71	59	36	-	-	-	-
Shiraishi[56]	55	74 ± 10	57	40	53	-	62	11	20	35	-
Makita[57]	94	69 ± 9	18	55	64	21	81	-	-	31	49
Miyagawa[58]	69	69 ± 5	33	54	55	59	80	-	27	16	38

CAD, coronary artery disease; *MI*, myocardial infarction; *Reva*, revascularization procedures

Table 4. Diagnostic performance in detecting coronary artery disease with CZT-SPECT camera

	True positive	False positive	True negative	False negative	Sensitivity (%)	Specificity (%)	Diagnostic odds ratio
Fiechter[44]	44	5	10	7	87	67	12.57
Duvall[45]	121	65	38	6	94.5	36.9	11.79
Duvall[46]	35	11	21	4	88.9	65.7	16.70
Chowdhury[47]	74	16	61	14	84	79	20.15
Perrin[48]	93	17	26	13	87	60	10.94
Nishiyama[49]	46	4	18	8	85	80	25.88
Barone-Rochette[50]	73	13	13	5	94	50	14.60
Mouden[51]	12	19	61	8	60	76	4.82
Gimelli[52]	406	115	139	35	92	54.7	14.02
Sharir[53]	127	14	51	16	90.6	78.1	28.92
Caobelli[54]	33	4	2	5	87	40	3.30
Liu[55]	27	46	130	8	76	74	9.54
Shiraishi[56]	12	9	32	2	83	77	21.33
Makita[57]	63	5	18	8	88.6	79.2	28.35
Miyagawa[58]	46	1	19	3	93.8	95	291.33

domains (patient selection, index test, and reference standard).

Diagnostic Accuracy of C-SPECT and CZT SPECT Cameras

The pooled sensitivity and specificity were 85% (95% CI 79-89) and 66% (95% CI 56-74) for C-SPECT (Figure 4) and 89% (95% CI 86-91) and 69% (95% CI 61-75) for CZT-SPECT (Figure 5) imaging studies. The summary ROC curves for C-SPECT and CZT-SPECT are depicted in Figures 6 and 7, respectively. The area under the curve was slightly higher for CZT-SPECT (0.89, 95% CI 0.86-0.92), with a rather restricted confidence and prediction regions, as compared to C-SPECT (0.83, 95% CI 0.80-0.86) ($P = .03$); accordingly, the summary diagnostic OR was 17 (95% CI 13-22) for CZT-SPECT and 11 (95% CI 7-15) for C-SPECT ($P = .04$). The accuracy of the two tests slightly differs between C-SPECT and CZT-SPECT (chi-square 11.28, 5 df, $P = .04$). However, we were unable to demonstrate if the subtle difference in global accuracy was due to sensitivity (chi-square 2.13, 1 df, $P = .14$) or specificity (chi-square 0.21, 1 df, $P = .65$), also when separate variances for each test were allowed in the models.

An additional analysis was performed excluding a C-SPECT study[43] with poor performance. The pooled sensitivity and specificity were 86 % (95% CI 81-89) and 65% (95% CI 56-74) for the remaining C-SPECT studies and the area under the curve (0.85, 95% CI 0.82-0.88) was still slightly lower ($P = .03$) as compared to CZT-SPECT.

Heterogeneity Analysis

Our analysis revealed that the heterogeneity in sensitivity was higher among C-SPECT (I^2 95.1%, $P < .001$) than CZT-SPECT (I^2 68.3%, $P < .001$) studies. Similarly, the heterogeneity in specificity was higher among C-SPECT (I^2 94.9%, $P < .001$) than CZT-SPECT (I^2 84.9%, $P < .001$) studies. The Spearman rank correlation test showed a weak threshold effect in C-SPECT studies (rho − 0.44, $P = .02$), but not in CZT-SPECT studies (rho − 0.32, $P = .23$).

Potential Bias and Meta-regression Analysis

The Deek's funnel plot shows a trend of asymmetry for C-SPECT (bias 6.49, standard error 3.30, $P = .06$) (Figure 8). Conversely, the Deek's funnel plot shows no evidence of asymmetry for CZT-SPECT (bias 2.29, standard error 4.77, $P = .64$) (Figure 9). At meta-regression analysis, no significant association between both sensitivity and specificity and demographic (age and gender) and clinical (diabetes, dyslipidemia,

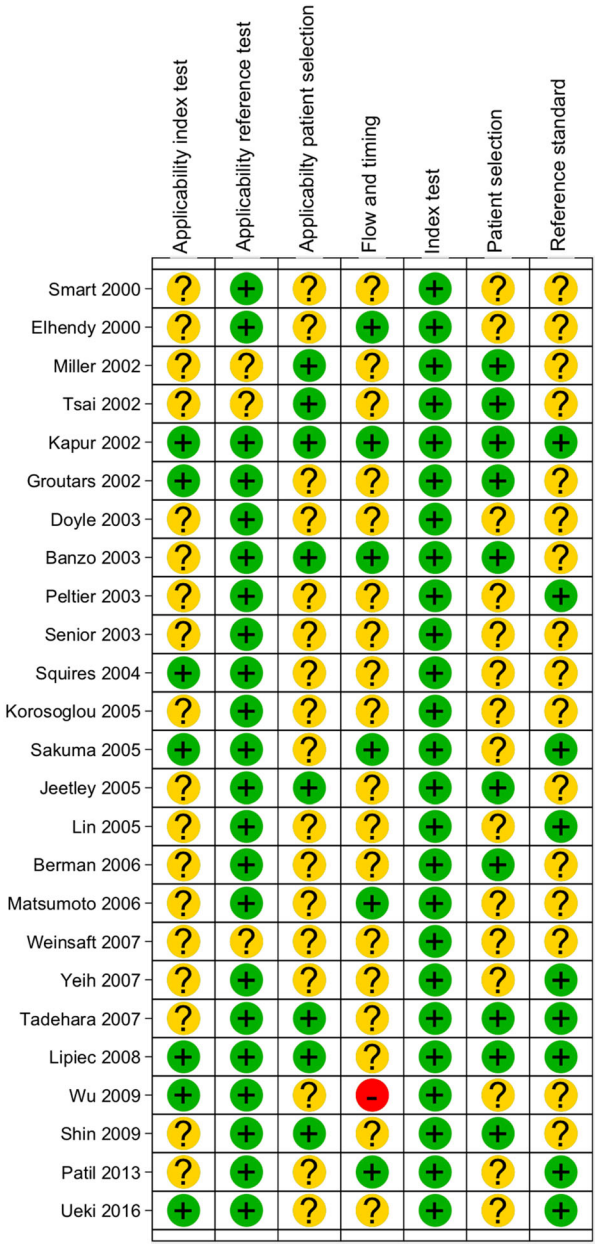

Figure 2. Methodological quality of the included C-SPECT studies assessed with QUADAS-2 tools for risk of bias and applicability concerns.

smoking, hypertension, angina-like symptom, and family history of CAD) variables considered was found for C-SPECT (Figure 10) and CZT-SPECT (Figure 11) studies. The prevalence of obstructive CAD was not different (P = .83) between C-SPECT (69%) and CZT-SPECT (53%) studies. Finally, the distribution of stenosis threshold and imaging tracers used were also not statistically different between C-SPECT and CZT-SPECT studies.

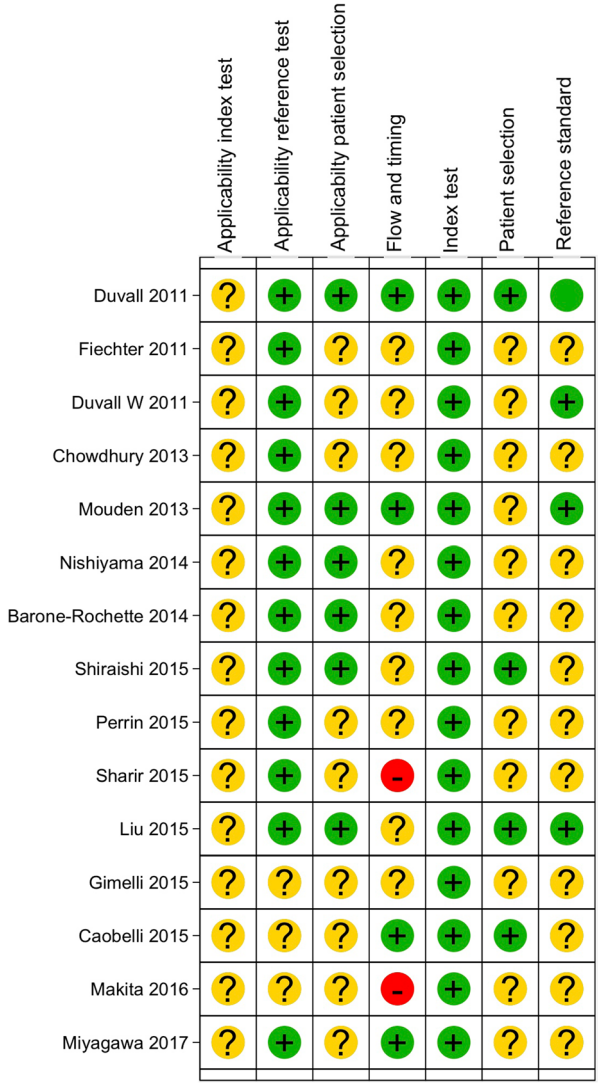

Figure 3. Methodological quality of the included CZT-SPECT studies assessed with QUADAS-2 tools for risk of bias and applicability concerns.

DISCUSSION

To our knowledge, this is the first meta-analysis comparing the diagnostic performance of C-SPECT and CZT-SPECT in detecting CAD in a large number of subjects undergoing stress MPI. We found a good diagnostic performance for the two gamma camera systems, with a slightly higher accuracy for CZT-SPECT.

MPI with SPECT is the most widely used nuclear cardiac imaging technique for the non-invasive assessment of cardiac disease including prognosis and choice of the most appropriate treatment strategies for patients with known or suspected CAD.[59,60] Nevertheless, drawbacks such as time-consuming acquisition, different

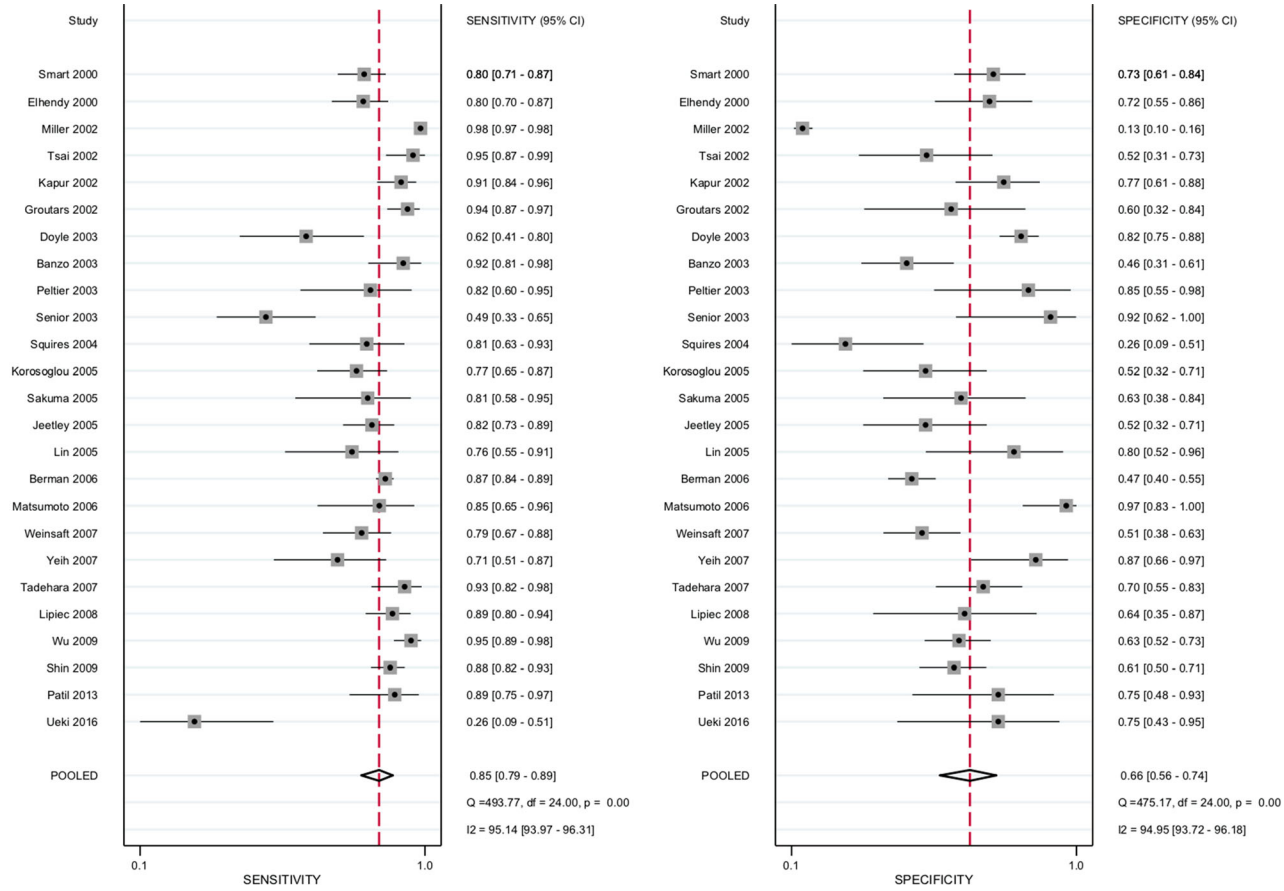

Figure 4. Forest plot of single studies for sensitivity and specificity for C-SPECT. Horizontal lines represent 95% confidence interval of the point estimates. Each solid circle represents sensitivity and specificity of individual studies, and the size of the circle indicates the study size. The diamond means the pooled sensitivity and specificity of all 25 studies. *CI*, confidence interval.

protocols, and radiation exposure still affect SPECT MPI. Refinements regarding iterative reconstruction algorithms,[61] early imaging protocols,[62] tracer development[24] and hardware equipment have been strengthened. Novel gamma cameras with semiconductor CZT detector technology have been introduced.[6] MPI acquired with CZT-SPECT has, compared to C-SPECT, an improved image quality but comparable diagnostic confidence.[63] Two studies have directly compared the performance of C-SPECT and CZT-SPECT in the same patient population.[5,64] Gimelli et al[64] demonstrated that CZT-SPECT was superior to C-SPECT for detecting global and regional ischemia and identified a higher number of vessels with obstructive CAD. In a multicenter study, Neill et al[5] reported similar results, with a superior sensitivity, specificity and accuracy (92%, 83% and 90% for CZT-SPECT vs 84%, 50% and 76% for C-SPECT).

To increase the level of validity of these results by combining data from multiple studies, we performed a meta-analysis of diagnostic test accuracy comparing indirectly CZT and C-SPECT studies. We identified 25 articles for C-SPECT and 15 articles for CZT-SPECT. The results showed that the accuracy of CZT-SPECT was slightly higher (P = .04) than that of C-SPECT; furthermore, the confidence and the prediction regions of summary ROC curve were narrower for CZT-SPECT than C-SPECT. The confidence region is based on the CI around the summery point and indicates that we would expect the 'real value' to be within that region 95% of the time. The prediction region around the summary point indicates the region where we would expect results from a new study in the future to lie.[17] Also, the diagnostic OR of CZT-SPECT was greater than that of C-SPECT, confirming that CZT-SPECT might be more accurate in assessing CAD. In fact, reflecting the combination of sensitivity and specificity, the diagnostic

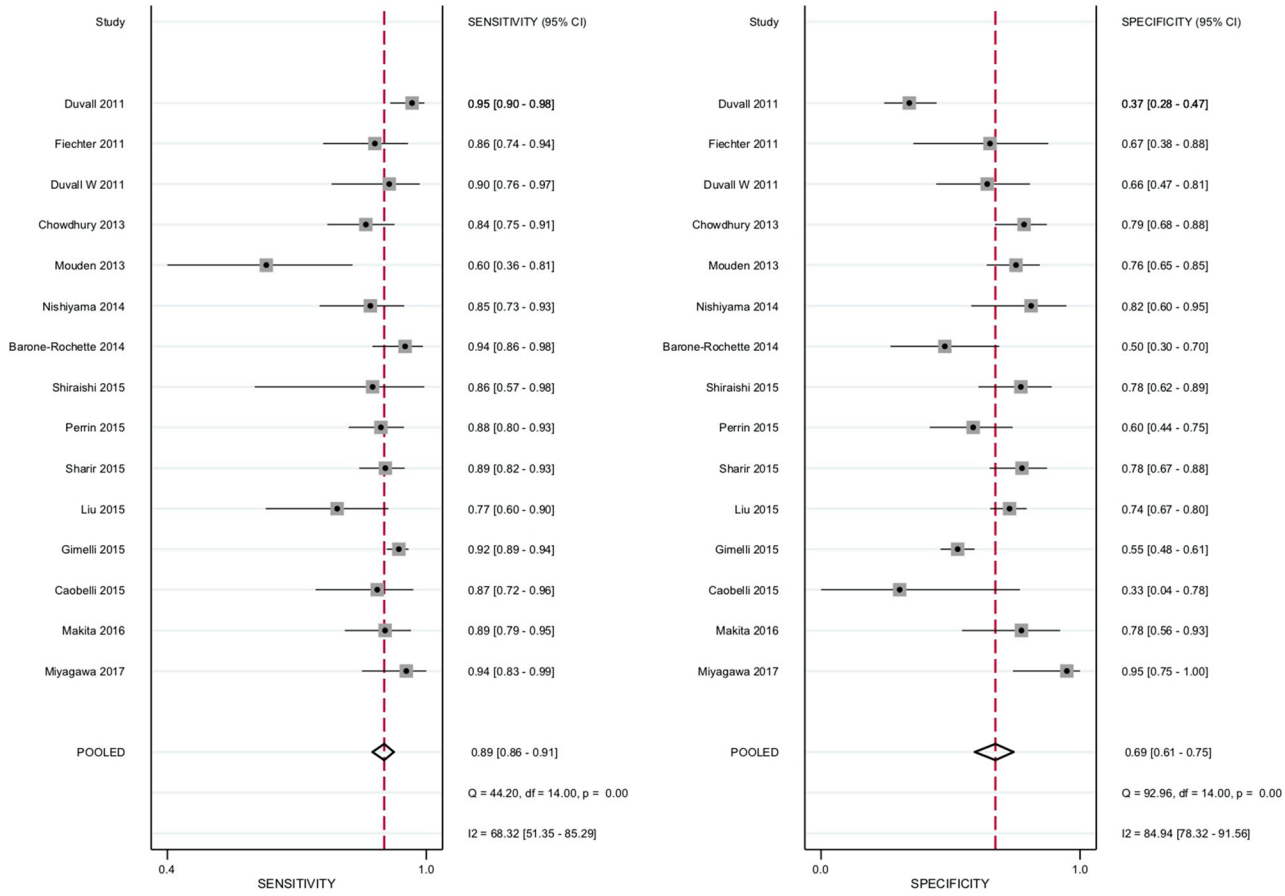

Figure 5. Forest plot of single studies for sensitivity and specificity for CZT SPECT. Horizontal lines represent 95% confidence interval of the point estimates. Each solid circle represents sensitivity and specificity of individual studies, and the size of the circle indicates the study size. The diamond means the pooled sensitivity and specificity of all 15 studies. *CI*, confidence interval.

OR can be regarded as a single measurement of diagnostic accuracy, with higher values indicate better discriminatory test performance.[65] Thus, our results suggest a slightly higher global accuracy of CZT-SPECT, also if the differences between pooled sensitivity and specificity of the two gamma cameras were not statistically significant, probably due to the high between study heterogeneity for both C-SPECT and CZT-SPECT studies. The additional analysis performed excluding a C-SPECT study[43] with poor performance showed that the area under the curve was still slightly lower as compared to that of CZT-SPECT. This result is not surprising, as Ueki et al[43] analyzed only 31 patients and the weight of this study did not affect considerably the result of the meta-analysis.

The slightly higher accuracy of CZT-SPECT may be explained by the better resolution and the better contrast and image quality of the solid-state camera as compared to the C-SPECT system. The shorter acquisition times and the novel camera design, allowing semi-upright acquisition with the patient's arms resting on the gantry, enhance patient comfort and potentially reduce the likelihood of motion artefacts. The short imaging time and potential to image a variety of radiotracers within 1 day allows flexibility in the choice of protocol, facilitating increased patient throughput. The intrinsic sensitivity of the system facilitates radioisotope dose reduction with a slight compromise on the length of acquisition time.[9,64] However, the performance of C-SPECT may be improved with software upgrading. Newer types of reconstruction software, such as wide beam reconstruction and ordered subset expectation maximization, have been proposed for MPI with C-SPECT systems.[66] These technologies reduce image noise by modeling it from spectral analysis of the projections, thereby improving image interpretation without affecting image resolution. These methods have already demonstrated

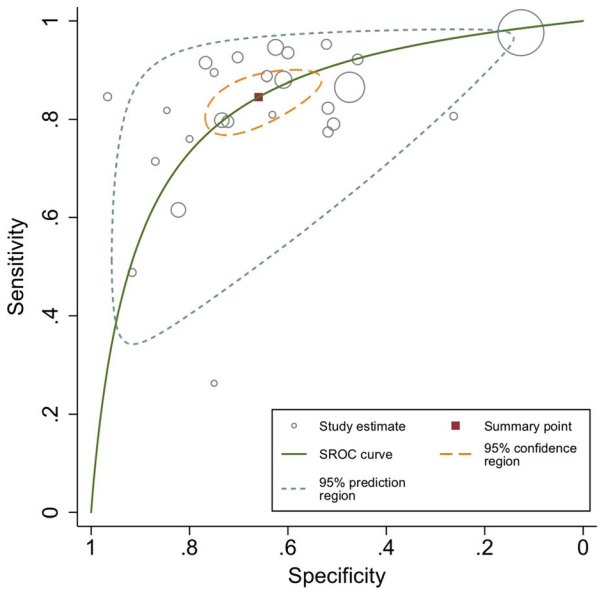

Figure 6. Summary receiver-operating characteristic curve for C-SPECT. Each circle represents individual study estimates. The diamond is the summary point representing the average sensitivity and specificity estimates. The ellipses around this summary point are the 95% confidence region (dashed line) and the 95% prediction region (dotted line). *AUC*, area under the curve; *SROC*, summary receiver-operating characteristic.

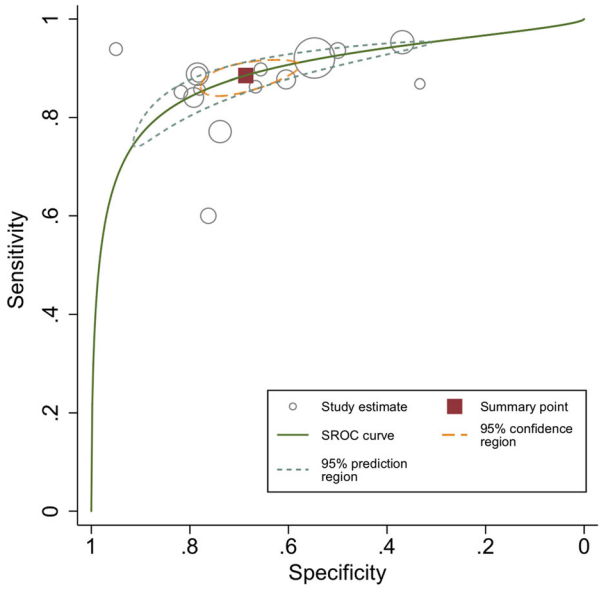

Figure 7. Summary receiver-operating characteristic curve for CZT SPECT. Each circle represents individual study estimates. The diamond is the summary point representing the average sensitivity and specificity estimates. The ellipses around this summary point are the 95% confidence region (dashed line) and the 95% prediction region (dotted line). *AUC*, area under the curve; *SROC*, summary receiver-operating characteristic.

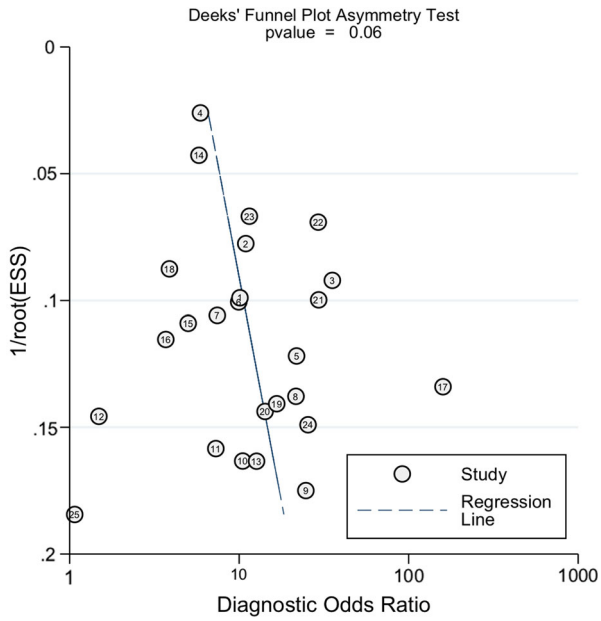

Figure 8. The Deeks' funnel plot asymmetry test for publication bias in the literature evaluation for C-SPECT. Each study is shown as a circle, and the regression line is shown by dashed line.

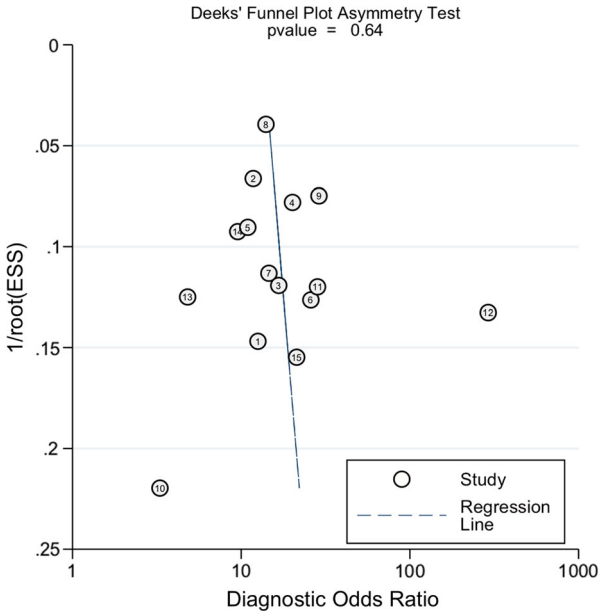

Figure 9. The Deeks' funnel plot asymmetry test for publication bias in the literature evaluation for CZT SPECT. Each study is shown as a circle, and the regression line is shown by dashed line.

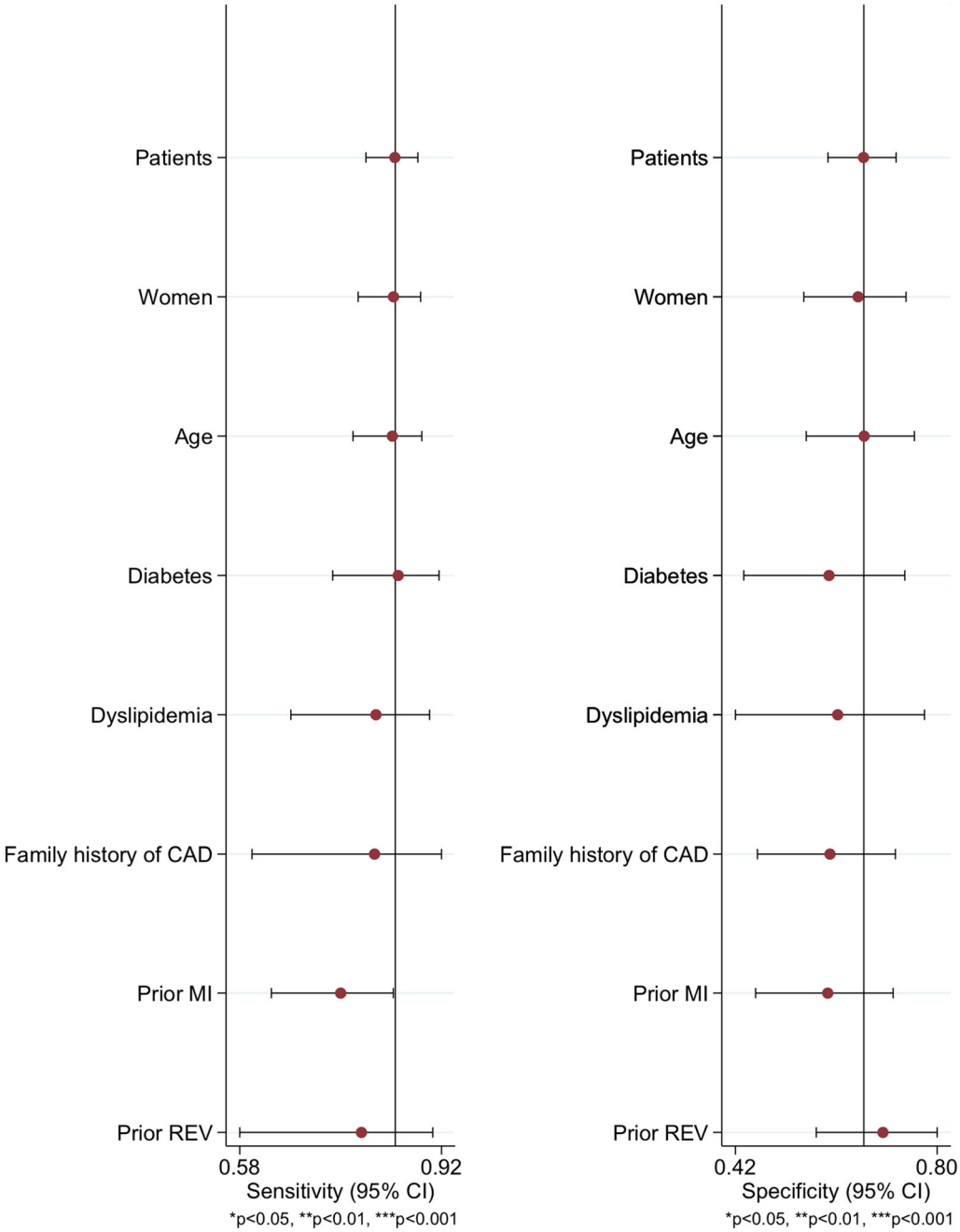

Figure 10. Forest plot of multiple univariable meta-regression and subgroup analyses for sensitivity and specificity of C-SPECT. Each solid circle represents sensitivity and specificity of studies considering covariates as the dependent variable and horizontal lines represent 95% confidence interval. *CI*, confidence interval.

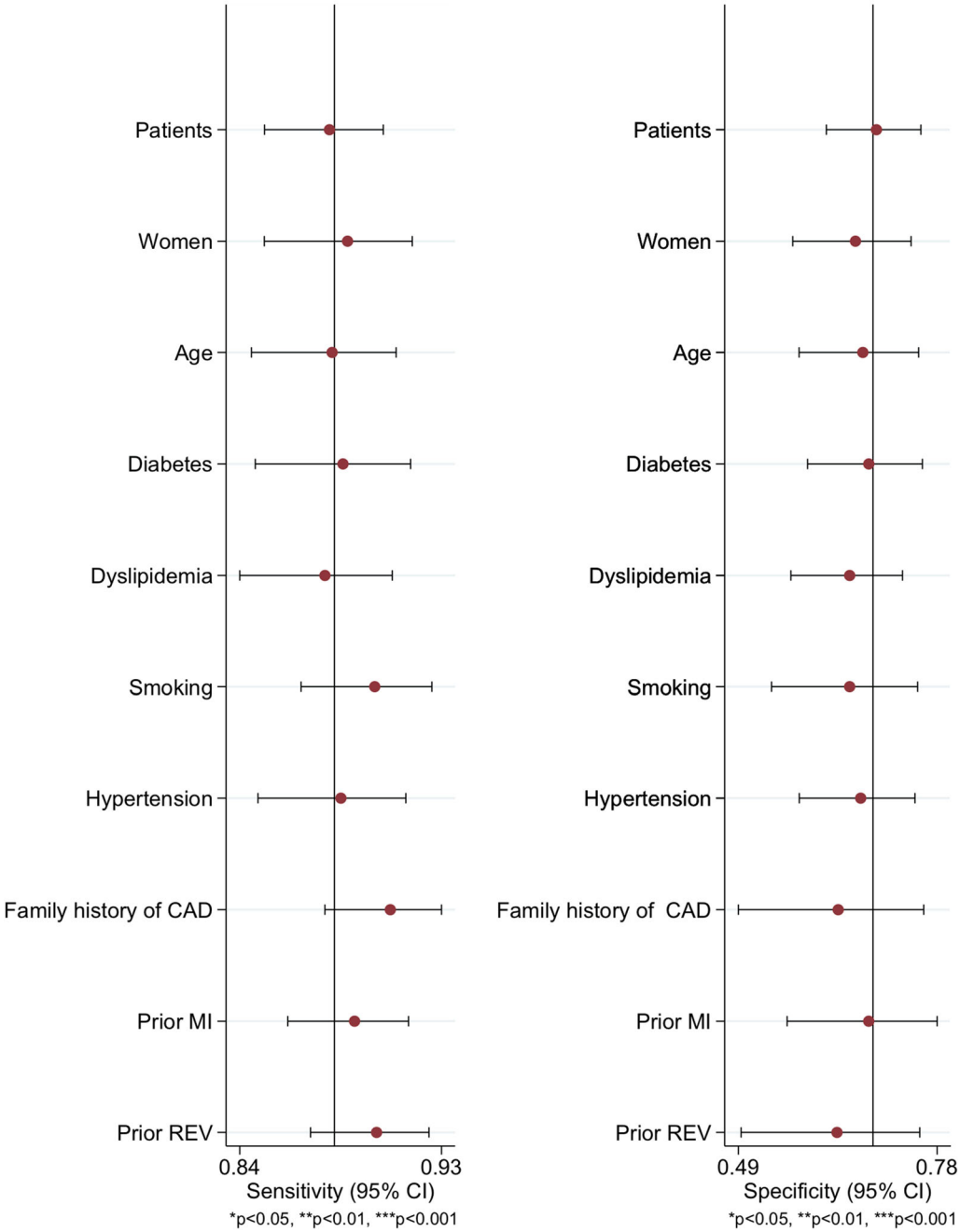

Figure 11. Forest plot of multiple univariable meta-regression and subgroup analyses for sensitivity and specificity of CZT SPECT. Each solid circle represents sensitivity and specificity of studies considering covariates as the dependent variable and horizontal lines represent 95% confidence interval. *CI*, confidence interval.

comparable performance and image quality of conventional filtered back projection method allowing though for half-time or half-dose MPI.

From our study, it emerged a trend of asymmetry in funnel plot among C-SPECT studies, suggesting the presence of bias. On the other hand, no significant asymmetry emerged in funnel plot among CZT-SPECT studies. Publication bias is a possible cause of funnel plot asymmetry. However, others possible sources are poor methodological quality, leading to spuriously inflated effects in smaller studies; true heterogeneity, in which the effects differ according to study size; and sampling variation, that can lead to an association between the effect and its standard error.[67]

Moreover, there was a greater heterogeneity for both sensitivity and specificity among C-SPECT than CZT-SPECT studies, attributed to differences in the spectrum of patients and to difference across studies in the choice of the cut-off of abnormality. As the statistical heterogeneity was substantial, we performed meta-regression to identify potential sources of bias.

At meta-regression analysis, we failed to find a significant search of heterogeneity associated with demographic and clinical characteristics for C-SPECT and CZT-SPECT studies. Hence, other confounding variables are the sources of the heterogeneity observed; therefore, we also performed the diagnostic threshold analysis to investigate the sources of heterogeneity.

LIMITATIONS

A limitation of our meta-analysis is that C-SPECT studies were over-represented and more than 50% of the included CZT-SPECT were published during the last ten years (from 2009). Another limitation is that differences in the distribution of study and patient characteristics potentially affecting the diagnostic performance of the imaging modalities. As regard the distribution of study quality, most studies gave a clear description of participants, index, and reference tests. However, the high number of items that were scored ''unclear'' was probably due to different study design. For instance, the risk of bias associated with patient selection domain was often attributed to studies including both subjects with known and suspected CAD. In addition, differences in demographic and clinical features among patients included in the primary studies might produce measures of diagnostic accuracy that vary considerably. As concern the flow and timing domain, the unclear risk of bias was primarily caused by the lack of an explicit description of the length of the time interval between the index test and the reference standard. Ideally, the results of the index test and the reference standard should be collected at the same time. Despite the presence of unclear items, the overall quality of the studies was reasonable to perform an adequate analysis. Finally, we performed an indirect comparison of the diagnostic value in detecting CAD of C-SPECT and CZT-SPECT due to the lack of head-to-head studies addressing the diagnostic performance by the two gamma cameras in the same patient population.

NEW KNOWLEDGE GAINED

The current study underscores the clinical use of the CZT-SPECT camera in detecting CAD as a valid replacement of conventional systems due to the important technological development of state-solid system.

CONCLUSION

The results of this meta-analysis indicate that C-SPECT and CZT-SPECT have good diagnostic performance in detecting angiographic proven CAD, with a slightly higher diagnostic accuracy of CZT-SPECT. This result supports the use of the novel gamma cameras in clinical routine practices also considering the improvements in acquisition time and radiation exposure reduction.

Disclosure

R Green, V. Cantoni, W. Acampa, E. Zampella, R. Assante, C. Nappi, V. Gaudieri, T. Mannarino, R. Cuocolo, E. Di Vaia, M. Petretta, A. Cuocolo declare that they have no conflict of interest.

References

1. Murray CJ, Lopez AD. Alternative projections of mortality and disability by cause 1990-2020: Global burden of disease study. Lancet 1997;349:1498-504.
2. Benjamin EJ, Virani SS, Callaway CW, Chamberlain AM, Chang AR, Cheng S, et al. Heart disease and stroke statistics-2018 update: A report from the American Heart Association. Circulation 2018;137:e67-492.
3. Gibbons RJ. Noninvasive diagnosis and prognosis assessment in chronic coronary artery disease: Stress testing with and without imaging perspective. Circ Cardiovasc Imaging 2008;1:257-69.
4. Green R, Cantoni V, Petretta M, Acampa W, Panico M, Buongiorno P, et al. Negative predictive value of stress myocardial perfusion imaging and coronary computed tomography angiography: A meta-analysis. J Nucl Cardiol 2018;25:1588-97.
5. Neill J, Prvulovich EM, Fish MB, Berman DS, Slomka PJ, Sharir T, et al. Initial multicenter experience of high-speed myocardial perfusion imaging: Comparison between high-speed and conventional single-photon emission computed tomography with angiographic validation. Eur J Nucl Med Mol Imaging 2013;40:1084-94.

6. Berman DS, Kang X, Tamarappoo B, Wolak A, Hayes SW, Nakazato R, et al. Stress thallium-201/rest technetium-99 m sequential dual isotope high-speed myocardial perfusion imaging. JACC Cardiovasc Imaging 2009;2:273-82.
7. Esteves FP, Raggi P, Folks RD, Keidar Z, Askew JW, Rispler S, et al. Novel solid-state-detector dedicated cardiac camera for fast myocardial perfusion imaging: Multicenter comparison with standard dual detector cameras. J Nucl Cardiol 2009;16:927-34.
8. Slomka PJ, Patton JA, Berman DS, Germano G. Advances in technical aspects of myocardial perfusion SPECT imaging. J Nucl Cardiol 2009;16:255-76.
9. Duvall WL, Croft LB, Ginsberg ES, Einstein AJ, Guma KA, George T, et al. Reduced isotope dose and imaging time with a high-efficiency CZT SPECT camera. J Nucl Cardiol 2011;18:847-57.
10. Herzog BA, Buechel RR, Katz R, Brueckner M, Husmann L, Burger IA, et al. Nuclear myocardial perfusion imaging with a cadmium-zinc-telluride detector technique: Optimized protocol for scan time reduction. J Nucl Med 2010;51:46-51.
11. Moher D, Liberati A, Tetzlaff J, Altman DG, PRISMA Group. Preferred reporting items for systematic reviews and meta-analyses: The PRISMA statement. PLoS Med 2009;6:e1000097.
12. Whiting PF, Rutjes AW, Westwood ME, Mallett S, Deeks JJ, Reitsma JB, et al. QUADAS-2: A revised tool for the quality assessment of diagnostic accuracy studies. Ann Intern Med 2011;155:529-36.
13. Reitsma JB, Glas AS, Rutjes AW, Scholten RJ, Bossuyt PM, Zwinderman AH. Bivariate analysis of sensitivity and specificity produces informative summary measures in diagnostic reviews. J Clin Epidemiol 2005;58:982-90.
14. Hanley JA, McNeil BJ. A method of comparing the areas under receiver operating characteristic curves derived from the same cases. Radiology. 1983;148:839-43.
15. Rosman AS, Korsten MA. Application of summary receiver operating characteristics (sROC) analysis to diagnostic clinical testing. Adv Med Sci 2007;52:76-82.
16. Van Houwelingen HC, Zwinderman KH. Stijnen T A bivariate approach to meta-analysis. Stat Med 1993;12:2273-84.
17. Takwoingi Y. Meta-analysis of test accuracy studies in Stata: A bivariate model approach. Version 1.1. April 2016. https://methods.cochrane.org/sdt/software-meta-analysis-dta-studies.
18. Lijmer JG, Mol BW, Heisterkamp S, Bonsel GJ, Prins MH, van der Meulen JH, et al. Empirical evidence of design-related bias in studies of diagnostic tests. JAMA 1999;282:1061-6.
19. Deeks JJ, Macaskill P, Irwig L. The performance of tests of publication bias and other sample size effects in systematic reviews of diagnostic test accuracy was assessed. J Clin Epidemiol 2005;58:882-93.
20. Elhendy A, Sozzi FB, Valkema R, van Domburg RT, Bax JJ, Roelandt JR. Dobutamine technetium-99m tetrofosmin SPECT imaging for the diagnosis of coronary artery disease in patients with limited exercise capacity. J Nucl Cardiol 2000;7:649-54.
21. Smart SC, Bhatia A, Hellman R, Stoiber T, Krasnow A, Collier BD, et al. Dobutamine-atropine stress echocardiography and dipyridamole sestamibi scintigraphy for the detection of coronary artery disease: Limitations and concordance. J Am Coll Cardiol 2000;36:1265-73.
22. Kapur A, Latus KA, Davies G, et al. A comparison of three radionuclide myocardial perfusion tracers in clinical practice: The ROBUST study. Eur J Nucl Med Mol Imaging. 2002;29:1608-16.
23. Miller TD, Hodge DO, Christian TF, Milavetz JJ, Bailey KR, Gibbons RJ. Effects of adjustment for referral bias on the sensitivity and specificity of single photon emission computed tomography for the diagnosis of coronary artery disease. Am J Med 2002;112:290-7.
24. Tsai MF, Kao PF, Tzen KY. Improved diagnostic performance of thallium-201 myocardial perfusion scintigraphy in coronary artery disease: From planar to single photon emission computed tomography imaging. Chang Gung Med J 2002;25:522-30.
25. Banzo I, Pena FJ, Allende RH, Quirce R, Carril JM. Prospective clinical comparison of non-corrected and attenuation- and scatter-corrected myocardial perfusion SPECT in patients with suspicion of coronary artery disease. Nucl Med Commun 2003;24:995-1002.
26. Doyle M, Fuisz A, Kortright E, Biederman RW, Walsh EG, Martin ET, et al. The impact of myocardial flow reserve on the detection of coronary artery disease by perfusion imaging methods: An NHLBI WISE study. J Cardiovasc Magn Reson 2003;5:475-85.
27. Groutars RG, Verzijlbergen JF, Tiel-van Buul MM, Zwinderman AH, Ascoop CA, van Hemel NM, et al. The accuracy of 1-day dual-isotope myocardial SPECT in a population with high prevalence of coronary artery disease. Int J Cardiovasc Imaging 2003;19:229-38.
28. Peltier M, Vancraeynest D, Pasquet A, Ay T, Roelants V, D'hondt AM, et al. Assessment of the physiologic significance of coronary disease with dipyridamole real-time myocardial contrast echocardiography. Comparison with technetium-99m sestamibi single-photon emission computed tomography and quantitative coronary angiography. J Am Coll Cardiol 2004;43:257-64.
29. Senior R, Lepper W, Pasquet A, Chung G, Hoffman R, Vanoverschelde JL, et al. Myocardial perfusion assessment in patients with medium probability of coronary artery disease and no prior myocardial infarction: Comparison of myocardial contrast echocardiography with 99mTc single-photon emission computed tomography. Am Heart J 2004;147:1100-5.
30. Sakuma H, Suzawa N, Ichikawa Y, Makino K, Hirano T, Kitagawa K, et al. Diagnostic accuracy of stress first-pass contrast-enhanced myocardial perfusion MRI compared with stress myocardial perfusion scintigraphy. AJR Am J Roentgenol 2005;185:95-102.
31. Squires SR, Bushnell DL, Menda Y, Graham MM. Comparison of cardiac to hepatic uptake of 99mTc-tetrofosmin with and without adenosine infusion to predict the presence of haemodynamically significant coronary artery disease. Nucl Med Commun 2005;26:513-8.
32. Lin SL, Chiou KR, Huang WC, Peng NJ, Tsay DG, Liu CP. Detection of coronary artery disease using real-time myocardial contrast echocardiography: A comparison with dual-isotope resting thallium-201/stress technectium-99m sestamibi single-photon emission computed tomography. Heart Vessels 2006;21:226-35.
33. Berman DS, Kang X, Nishina H, Slomka PJ, Shaw LJ, Hayes SW, et al. Diagnostic accuracy of gated Tc-99m sestamibi stress myocardial perfusion SPECT with combined supine and prone acquisitions to detect coronary artery disease in obese and non-obese patients. J Nucl Cardiol 2006;13:191-201.
34. Jeetley P, Hickman M, Kamp O, Lang RM, Thomas JD, Vannan MA, et al. Myocardial contrast echocardiography for the detection of coronary artery stenosis: A prospective multicenter study in comparison with single-photon emission computed tomography. J Am Coll Cardiol 2006;47:141-5.
35. Korosoglou G, Dubart AE, DaSilva KG Jr, Labadze N, Hardt S, Hansen A, et al. Real-time myocardial perfusion imaging for pharmacologic stress testing: Added value to single photon emission computed tomography. Am Heart J 2006;151:131-8.
36. Matsumoto N, Sato Y, Suzuki Y, Yoda S, Kunimasa T, Kato M, et al. Usefulness of rapid low-dose/high-dose 1-day 99mTc-

sestamibi ECG-gated myocardial perfusion single-photon emission computed tomography. Circ J 2006;70:1585-9.
37. Weinsaft JW, Gade CL, Wong FJ, Kim HW, Min JK, Manoushagian SJ, et al. Diagnostic impact of SPECT image display on assessment of obstructive coronary artery disease. J Nucl Cardiol 2007;14:659-68.
38. Yeih DF, Huang PJ, Ho YL. Enhanced diagnosis of coronary artery disease in women by dobutamine thallium-201 ST-segment/heart rate slope and thallium-201 myocardial SPECT. J Formos Med Assoc 2007;106:832-9.
39. Lipiec P, Wejner-Mik P, Krzemińska-Pakuła M, Kuśmierek J, Płachcińska A, Szumiński R, et al. Accelerated stress real-time myocardial contrast echocardiography for the detection of coronary artery disease: Comparison with 99mTc single photon emission computed tomography. J Am Soc Echocardiogr 2008;21:941-7.
40. Tadehara F, Yamamoto H, Tsujiyama S, Hinoi T, Matsuo S, Matsumoto N, et al. Feasibility of a rapid protocol of 1-day single-isotope rest/adenosine stress Tc-99m sestamibi ECG-gated myocardial perfusion imaging. J Nucl Cardiol 2008;15:35-41.
41. Wu MC, Chin KC, Lin KH, Chiu NT. Diagnostic efficacy of a low-dose 32-projection SPECT 99mTc-sestamibi myocardial perfusion imaging protocol in routine practice. Nucl Med Commun 2009;30:140-7.
42. Shin JH, Pokharna HK, Williams KA, Mehta R, Ward RP. SPECT myocardial perfusion imaging with prone-only acquisitions: Correlation with coronary angiography. J Nucl Cardiol 2009;16:590-6.
43. Patil HR, Bateman TM, McGhie AI, Burgett EV, Courter SA, Case JA, et al. Diagnostic accuracy of high-resolution attenuation-corrected Anger-camera SPECT in the detection of coronary artery disease. J Nucl Cardiol 2014;21:127-34.
44. Ueki Y, Izawa A, Kashiwagi D, Nishiyama S, Aso S, Suzuki C, et al. Diagnostic advantage of stress computed tomography myocardial perfusion over single-photon emission computed tomography for the assessment of myocardial ischemia. J Cardiol 2017;70:147-54.
45. Fiechter M, Ghadri JR, Kuest SM, Pazhenkottil AP, Wolfrum M, Nkoulou RN, et al. Nuclear myocardial perfusion imaging with a novel cadmium-zinc-telluride detector SPECT/CT device: First validation versus invasive coronary angiography. Eur J Nucl Med Mol Imaging 2011;38:2025-30.
46. Duvall WL, Sweeny JM, Croft LB, Barghash MH, Kulkarni NK, Guma KA, et al. Comparison of high efficiency CZT SPECT MPI to coronary angiography. J Nucl Cardiol 2011;18:595-604.
47. Duvall WL, Sweeny JM, Croft LB, Ginsberg E, Guma KA, Henzlova MJ. Reduced stress dose with rapid acquisition CZT SPECT MPI in a non-obese clinical population: Comparison to coronary angiography. J Nucl Cardiol 2012;19:19-27.
48. Chowdhury FU, Vaidyanathan S, Bould M, Marsh J, Trickett C, Dodds K, et al. Rapid-acquisition myocardial perfusion scintigraphy (MPS) on a novel gamma camera using multipinhole collimation and miniaturized cadmium-zinc-telluride (CZT) detectors: Prognostic value and diagnostic accuracy in a 'real-world' nuclear cardiology service. Eur Heart J Cardiovasc Imaging 2014;15:275–83.
49. Perrin M, Djaballah W, Moulin F, Claudin M, Veran N, Imbert L, et al. Stress-first protocol for myocardial perfusion SPECT imaging with semiconductor cameras: High diagnostic performances with significant reduction in patient radiation doses. Eur J Nucl Med Mol Imaging 2015;42:1004-11.
50. Nishiyama Y, Miyagawa M, Kawaguchi N, Nakamura M, Kido T, Kurata A, et al. Combined supine and prone myocardial perfusion single-photon emission computed tomography with a cadmium zinc telluride camera for detection of coronary artery disease. Circ J 2014;78:1169-75.
51. Barone-Rochette G, Leclere M, Calizzano A, Vautrin E, Céline GC, Broisat A, et al. Stress thallium-201/rest technetium-99m sequential dual-isotope high-speed myocardial perfusion imaging validation versus invasive coronary angiography. J Nucl Cardiol 2015;22:513-22.
52. Gimelli A, Liga R, Duce V, Kusch A, Clemente A, Marzullo P. Accuracy of myocardial perfusion imaging in detecting multivessel coronary artery disease: A cardiac CZT study. J Nucl Cardiol 2017;24:687-95.
53. Sharir T, Pinskiy M, Pardes A, Rochman A, Prokhorov V, Kovalski G, et al. Comparison of the diagnostic accuracies of very low stress-dose with standard-dose myocardial perfusion imaging: Automated quantification of one-day, stress-first SPECT using a CZT camera. J Nucl Cardiol 2016;23:11-20.
54. Caobelli F, Akin M, Thackeray JT, Brunkhorst T, Widder J, Berding G, et al. Diagnostic accuracy of cadmium-zinc-telluride-based myocardial perfusion SPECT: Impact of attenuation correction using a co-registered external computed tomography. Eur Heart J Cardiovasc Imaging 2016;17:1036-43.
55. Makita A, Matsumoto N, Suzuki Y, Hori Y, Kuronuma K, Yoda S, et al. Clinical feasibility of simultaneous acquisition rest (99m)Tc/stress (201)Tl dual-isotope myocardial perfusion single-photon emission computed tomography with semiconductor camera. Circ J 2016;80:689-95.
56. Miyagawa M, Nishiyama Y, Uetani T, Ogimoto A, Ikeda S, Ishimura H, et al. Estimation of myocardial flow reserve utilizing an ultrafast cardiac SPECT: Comparison with coronary angiography, fractional flow reserve, and the SYNTAX score. Int J Cardiol 2017;244:347-53.
57. Mouden M, Ottervanger JP, Knollema S, Timmer JR, Reiffers S, Oostdijk AH, et al. Myocardial perfusion imaging with a cadmium zinc telluride-based gamma camera versus invasive fractional flow reserve. Eur J Nucl Med Mol Imaging 2014;41:956-62.
58. Liu CJ, Wu YW, Ko KY, Chen YC, Cheng MF, Yen RF, et al. Incremental diagnostic performance of combined parameters in the detection of severe coronary artery disease using exercise gated myocardial perfusion imaging. PLoS ONE 2015;10:e0134485.
59. Shiraishi S, Sakamoto F, Tsuda N, Yoshida M, Tomiguchi S, Utsunomiya D, et al. Prediction of left main or 3-vessel disease using myocardial perfusion reserve on dynamic thallium-201 single-photon emission computed tomography with a semiconductor gamma camera. Circ J 2015;79:623-31.
60. Megna R, Zampella E, Assante R, Nappi C, Gaudieri V, Mannarino T, et al. Temporal trends of abnormal myocardial perfusion imaging in a cohort of Italian subjects: Relation with cardiovascular risk factors. J Nucl Cardiol 2019. https://doi.org/10.1007/s12350-019-01630-1.
61. Thomas GS, Miyamoto MI, Morello AP, Majmundar H, Thomas JJ, Sampson CH, et al. Technetium 99m sestamibi myocardial perfusion imaging predicts clinical outcome in the community outpatient setting. The nuclear utility in the Community (NUC) study. J Am Coll Cardiol 2004;43:213-23.
62. Seo Y, Mari C, Hasegawa BH. Technological development and advances in single-photon emission computed tomography/computed tomography. Semin Nucl Med 2008;38:177-98.
63. Giorgetti A, Rossi M, Stanislao M, Valle G, Bertolaccini P, Maneschi A, et al. Feasibility and diagnostic accuracy of a gated SPECT early-imaging protocol: A multicenter study of the Myoview Imaging Optimization Group. J Nucl Med 2007;48:1670-5.

64. Agostini D, Marie PY, Ben-Haim S, Rouzet F, Songy B, Giordano A, et al. Performance of cardiac cadmium-zinc-telluride gamma camera imaging in coronary artery disease: A review from the cardiovascular committee of the European Association of Nuclear Medicine (EANM). Eur J Nucl Med Mol Imaging 2016;43:2423-32.
65. Sterne JA, Sutton AJ, Ioannidis JP, Terrin N, Jones DR, Lau J, et al. Recommendations for examining and interpreting funnel plot asymmetry in meta-analyses of randomized controlled trials. BMJ 2011;343:4002.
66. Gimelli A, Bottai M, Giorgetti A, Genovesi D, Kusch A, Ripoli A, et al. Comparison between ultrafast and standard SPECT in patients with coronary artery disease: A pilot study. Circul Cardiovasc Imag 2011;4:51-8.
67. Glas AS, Lijmer JG, Prins MH, Bonsel GJ, Bossuyt PM. The diagnostic odds ratio: A single indicator of test performance. J Clin Epidemiol 2003;56:1129-35.